Polymer 50 (2009) 1645–1653

Contents lists available at ScienceDirect

Polymer

journal homepage: www.elsevier.com/locate/polymer

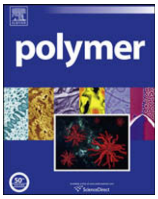

Covalent attachment of chromophores to chlorinated copolymers for optical waveguides: Synthesis and optical characterization

Pierfrancesco Cerruti [a,*], Fabio Borbone [b], Antonio Carella [b], Mario Malinconico [a], Pasquale Mormile [c], Lucia Petti [c], Massimo Rippa [c], Antonio Roviello [b], Paola Laurienzo [a,**]

[a] *Institute of Polymer Chemistry and Technology, CNR, Via Campi Flegrei 34, 80078 Pozzuoli (Naples), Italy*
[b] *Department of Chemistry Paolo Corradini, University of Naples Federico II, Via Cinthia, 80126 Naples, Italy*
[c] *Institute of Cybernetics Eduardo Caianiello, CNR, Via Campi Flegrei 34, 80078 Pozzuoli (Naples), Italy*

ARTICLE INFO

Article history:
Received 25 November 2008
Received in revised form
30 January 2009
Accepted 1 February 2009
Available online 7 February 2009

Keywords:
Chlorostyrene–glycidyl methacrylate copolymer
Photoinitiated crosslinking
Optical waveguides

ABSTRACT

Polymeric optical devices are attracting increasing interest in the field of photonics because of the very appealing performances as structures for both propagating and modulating light signals according to the properties of the employed organic materials. This paper reports the preparation and characterization of low-loss polymer waveguides fabricated from chlorinated copolymers by photochemical crosslinking. A novel monomer derived from reaction between glycidyl methacrylate (GMA) and the chromophore Disperse Red 19 (DR19) was prepared and successfully copolymerized with GMA and chlorostyrene (CS) to obtain the dye-modified copolymer. The latter was crosslinked by photoinitiated polymerization of the pendant epoxy groups, to obtain stable polymeric waveguides. It was found that the major product of the reaction between GMA and DR19 was formed through transesterification of the methacrylate with elimination of glycidol, while traces of products deriving from the epoxy ring-opening reaction were detected. The presence of the nitro substituent on DR19 favoured chain-transfer reactions during the polymerization reaction, leading to a decrease in the polymerization degree. It was also observed that the presence of grafted DR19 negatively affected the crosslinking reaction, as a lower epoxy group conversion was observed for the modified copolymer. Thermal analysis showed increased thermal stability for the copolymer containing DR19. *m-line* spectroscopy was used to measure the refractive index at 632.8 nm. The experimental results confirm that the new class of chlorine-based polymeric materials represent a very attractive proposal in the panorama of materials employed in the fabrication of electro-optical devices for telecommunication applications.

© 2009 Elsevier Ltd. All rights reserved.

1. Introduction

In the last two decades polymeric guiding structures are attracting more and more attention for the potential applications in various fields ranging from photonics to integrated optics and telecommunication. For instance, organic materials have been designed for electroluminescence [1–3], nonlinear optics [4,5], signal amplifiers [6,7], optical fibers [8,9] and passive waveguides [10–12]. Polymers for passive optical waveguiding can be made with low-cost, flexible manufacturing techniques that can be applied to a variety of substrates, giving different design possibilities for integrated optical circuits as board-to-board connections, splitters, couplers, and filters. In terms of device performance, such materials have to combine high transparency in the near-IR regime, controlled refractive index, good optical properties at temperatures greater than 200 °C, high mechanical flexibility, long-term stability and ease of processing. Their optical properties, such as refractive index and optical losses, can be tailored to the specific requirements of the application through chemical synthesis. By electric poling, active electro-optical polymers are obtained that use the linear electro-optic Pockels effect occurring in noncentrosymmetric χ^2 materials.

The achievement of good optical loss performances can be accomplished by reducing the number of chemical linkages, such as C–H, O–H, N–H, which strongly absorb in the near-IR. Substitution of hydrogen atoms with heavier elements, such as halogens, shifts the absorption range to longer wavelengths. Several literature reports describe the use of halogenated polymers suitable to be employed as thermally stable, low-loss optical waveguides. Copolymers based on pentafluorostyrene (PFS) and 4-chlorostyrene (CS) containing

---

* Corresponding author. Tel.: +39 0818675214; fax: +39 0818675230.
** Corresponding author. Tel.: +39 0818675215; fax: +39 0818675230.
E-mail addresses: cerruti@unina.it (P. Cerruti), paola.laurienzo@ictp.cnr.it (P. Laurienzo).

0032-3861/$ – see front matter © 2009 Elsevier Ltd. All rights reserved.
doi:10.1016/j.polymer.2009.02.001

glycidyl methacrylate (GMA) as a photocrosslinkable comonomer were prepared to increase thermal stability and provide long-lasting optical properties [13–17].

Due to their aliphatic backbone, these polymers have a low absorption in the ultraviolet (UV) region, and therefore their optical characteristics are difficult to monitor by means of UV–vis spectroscopy. To overcome this drawback, UV-absorbing dyes are usually added in the polymer formulation. These chromophores may also increase thermal stability and induce noncentrosymmetric characteristics in the material [18,19].

Among the several classes of chromophores, azobenzene dyes have found many applications in recent years, which exploit their property of photoisomerization [20]. The reversible *cis–trans* isomerization can lead to differences in absorption spectra, dipole moments, refraction indexes, which can be used in optical storage [21,22]. Besides, azobenzene groups are dipole nonlinear optical chromophores that may be employed for the synthesis of electro-optical polymer materials designed for broadband light modulators and integral optoelectronic chips [23].

One strategy widely employed to obtain incorporation of azo dyes in polymer is to prepare guest–host solutions in which the dye is physically dispersed within the polymer matrix [14,24–26]. However, these systems are generally considered unsuitable for applications, due to loss of alignment stability, the plasticizing effect of the guest chromophores that may lower the glass transition temperature (T_g), and the possibility of phase separation at high dye loading.

Covalent attachment of the chromophore to polymer backbone is seen as an effective means to provide long-term stability in optical anisotropy as well as to minimize near-IR absorption loss [27].

Azochromophores may be incorporated into a polymer matrix via condensation reactions [28–30], or radical (co)polymerization [23,31,32]. The latter has been often achieved by chemical modification of the chromophore with methacryloyl groups, which were then copolymerized alongside other acrylic monomers. Methacrylated chromophores are usually prepared through the interaction of methacryloyl chloride with the chromophore molecule. However, drawbacks in this method are related to the evolution of hydrogen chloride in the course of reaction causing a potential decrease in the efficiency of dipole polarization of the resulting material [23]. One way to overcome this problem is to replace chloride with other acrylates bearing reactive groups, such as epoxy ring in GMA [33,34]. An additional advantage of using GMA as a co-monomer is the possibility of facile chemical crosslinking of the resulting polymer through epoxy groups by means of photo-induced polymerization at relatively low temperatures, without excluding oxygen from air [35–38].

In the present paper we report on the synthesis, molecular characterization and preliminary optical measurements of a copolymer based on CS, GMA, and an acrylic monomer bearing an azobenzene chromophore (DR19) in the side chain. The latter has been obtained through chemical reaction between GMA and DR19, in the presence of suitable catalysts. A low-loss polymer waveguide was fabricated by spin-coating and photo-crosslinking the copolymer onto a glass slide. To investigate on the influence of the chromophore on polymer behaviour, the physico-chemical properties of the azo dye-modified polymer were compared to those of the plain poly(**CS**–**GMA**).

2. Experimental

2.1. Materials

DR19 was prepared as already reported [39]. 4-Chlorostyrene (CS) and glycidyl methacrylate (GMA) were purchased from Aldrich Chemical Co. and purified by low-pressure distillation over molecular sieves. Benzoyl peroxide (BPO), acetone, *n*-hexane, dichloromethane (CH_2Cl_2), *N,N*-dimethylformamide (DMF), tetrahydrofuran (THF), 4-dimethylaminopyridine (DMAP), boron trifluoride-diethyl etherate (BFEt), ethyltriphenylphosphonium bromide (ETPP), and titanium tetrabutoxide (TiBuO) were purchased from Aldrich and used as-received. Cyracure UVI 6974 (a mixture of arylsulfonium hexafluoroantimonates at 50 wt% in propylene carbonate) was kindly supplied by Dow Chemicals.

2.2. Synthesis of the dye-modified monomer 4′-[N-(2-hydroxyethyl)-N-(2-methacryloxyethyl)amino]-4-nitroazobenzene (**MA19**)

A round bottom flask equipped with a stirrer and a condenser was charged with GMA (1.43 g, 10 mmol), DR19 (3.30 g, 10 mmol), DMAP (1.22 g, 10 mmol) and 20 ml of DMF. The resulting mixture was kept at 80 °C for 12 h. The solvent was then evaporated and the product mixture obtained was purified by column chromatography on silica gel (Merck, Silica gel 60), using CH_2Cl_2 as eluting agent. After evaporation of the solvent, **MA19** was obtained as a red solid. The yield of the product was 48%.

^{1}H NMR ($CDCl_3$), δ (ppm): 8.34 (d, $J = 9.3$ Hz, 2H), 7.92 (m, $J = 9.3$ Hz, 4H), 6.88 (d, $J = 9.3$ Hz, 2H), 6.10 (s, 1H), 5.59 (t, $J = 1.2$ Hz, 1H), 4.44 (t, $J = 6.0$ Hz, 2H), 3.92 (m, $J = 5.3$ Hz, 2H,), 3.85 (t, $J = 6.0$ Hz, 2H), 3.70 (t, $J = 5.3$ Hz, 2H), 1.93 (s, 3H), 1.88 (t broad, $J = 5.4$ Hz, 1H).

2.3. Preparation of poly(4-chlorostyrene-co-glycidylmethacrylate) (poly(**CS**–**GMA**))

The synthetic procedure was adapted from [15]. Briefly, a round bottom flask equipped with a stirrer and a condenser was charged with 30.44 g of CS (224 mmol), 7.94 g of GMA (56.0 mmol) and 274.0 mg of BPO (1.14 mmol) in THF (70 ml). The resulting solution was degassed by a freeze–thaw process using liquid nitrogen, then kept at 70 °C for 24 h. The solution was then cooled to room temperature, poly(**CS**–**GMA**) was precipitated in *n*-hexane and purified by dissolution in CH_2Cl_2 and reprecipitation in hexane. The polymer was vacuum-dried at 60 °C. Approximately 20 g of product was collected (yield: 52%).

^{13}C NMR ($CDCl_3$), δ (ppm): 175.7, 143.0, 131.8, 128.7, 64.6, 48.9, 45.5, 44.2, 39.9, 38.5, 20.2.

^{1}H NMR ($CDCl_3$), δ (ppm): 7.08 (broad s, aromatic, CS), 6.55 (m, aromatic, CS), 4.06–3.13 (m overlapped, $-OCH_2-$ in GMA, $>$CH– of epoxy ring in GMA), 2.73–2.24 (m, $-CH_2-$ of epoxy ring of GMA), 1.82 (m, $>$CH– of CS), 1.56–1.25 (m, $-CH_2-$ in backbone), 0.89–0.49 (m, $-CH_3$ of GMA) [40].

2.4. Preparation of the terpolymer poly(4-chlorostyrene-co-glycidylmethacrylate-co-MA19) (poly(**CS**–**GMA**–**MA19**))

A round bottom flask equipped with a stirrer and a condenser was charged with 5.06 g of CS (37.2 mmol), 1.22 g of GMA (8.6 mmol), 0.28 g of **MA19** (0.63 mmol) and 100.0 mg of BPO (0.42 mmol) in THF (20 ml). The polymerization and the subsequent work-up of the reaction mixture were carried out as described for poly(**CS**–**GMA**) yielding 2.1 g of poly(**CS**–**GMA**–**MA19**) (32%).

^{13}C NMR ($CDCl_3$), δ (ppm): 175.7, 143.0, 131.8, 128.7, 126.1, 124.7, 122.7, 111.8, 65.0, 53.4, 48.9, 45.5, 44.2, 39.9, 38.5, 20.2.

^{1}H NMR ($CDCl_3$), δ (ppm): 8.33 (m, aromatic, *ortho* to $-NO_2$ in MA19), 7.94 (m, aromatic, *ortho* to $-N{=}N-$ in MA19), 7.08 (broad s, aromatic), 6.55 (m, aromatic), 4.06–3.13 (m overlapped, $-OCH_2-$ in

GMA, >CH– of epoxy ring in GMA), 2.73–2.24 (m, $–CH_2–$ of epoxy ring of GMA), 1.82 (m, >CH– of CS), 1.56–1.25 (m, $–CH_2–$ in backbone), 0.89–0.49 (m, $–CH_3$ of GMA).

2.5. Waveguide fabrication

Optical waveguides were fabricated by spin-coating onto glass slides the polymer solution containing a photoinitiator able to catalyze thermal crosslinking of the polymer by cationic polymerization of the oxirane residues on the GMA moieties. The photoinitiator used for UV-activated crosslinking was a mixture of arylsulfonium hexafluoroantimonates (UVI 6974 from Union-Carbide).

Poly(**CS**–**GMA**–**MA19**) was dissolved in chloroform (10 wt%), and the photoinitiator (1 wt%) was added. The resulting solution was filtered through a 0.2 μm Teflon membrane filter and then spin-coated (Karl Suss RC5) onto fused silica slides. The coated slides were heated at 70 °C to allow solvent evaporation, then were UV-irradiated with a Hg–Xe high pressure lamp (200 mJ/cm^2) for 5 min, and finally cured at 130 °C for 75 min. The thickness of the prepared waveguides varied from 1 μm to 1.4 μm according to the different spinning parameters. In particular, spinning rate varied from 600 to 800 rpm with a controlled acceleration of 100 rpm/s to obey to the designing requirements.

2.6. Characterization techniques

DSC measurements were performed on a Mettler–Toledo DSC 30 calorimeter, using 10 mg of polymer powder. All polymer samples were heated under nitrogen from 0 to 180 °C, cooled to 0 °C, and then reheated to 250 °C using a scan rate of 10 °C/min. Glass transition temperatures were evaluated from the second heating scan.

TG measurements were carried out at 10 °C/min heating rates from 30 to 800 °C in nitrogen (flow rate 100 ml/min) on approximately 10 mg polymer by means of a Perkin Elmer Pyris Diamond TG–DTA. To eliminate small amounts of water absorbed, a 30-minute isothermal treatment at 90 °C was carried out prior to heating.

The number-average molecular weight (M_n) and weight-average molecular weight (M_w) of the polymers were estimated by gel permeation chromatography (GPC) (Waters 410, polystyrene standards calibration) in THF.

^1H and ^{13}C NMR spectra were obtained on a Bruker AVANCE 300 MHz NMR spectrometer. Chemical shifts are reported in ppm: s = singlet, d = doublet, t = triplet, m = multiplet.

Ultraviolet–visible (UV–vis) absorption spectra were measured on a Jasco V-570 spectrophotometer.

Transmission infrared (FTIR) spectra of polymer films cast on KBr discs were obtained using a System 2000 spectrometer from Perkin–Elmer, collecting 16 scans at a resolution of 4 cm^{-1}. FTIR spectroscopy was also used to measure the crosslinking kinetics of the polymers. A film of each uncured polymer, containing 1 wt% of UVI 6974, was cast onto a KBr disc. After solvent evaporation the disc was UV-irradiated for 5 min and then collocated in a pre-heated (T = 130 °C), nitrogen purged, environmental chamber directly fitted in the spectrometer. The chamber was self-constructed by modifying the commercially available SPECAC 20100 cell. This unit was controlled by an Eurotherm PID temperature controller model 2416, with an accuracy of ±0.5 °C, The ratios of the areas under the 912 cm^{-1} epoxy ring peak and the 830 cm^{-1} constant peak (used as an internal standard) of the aromatic rings in the polymers, represent a relative measure of the curing degree [31,41].

3. Results and discussion

3.1. Preparation and characterization of **MA19**

The synthesis of the **MA19** was achieved through the condensation between DR19 and GMA. The expected reaction pathway involved the ring-opening reaction of glycidyl groups of GMA by hydroxyl groups of DR19, or the transesterification of the methacrylate with elimination of glycidol (Scheme 1). Both reaction products were suitable to be copolymerized with unsaturated acrylic monomers.

An attempt to get any product by uncatalyzed reaction of DR19 with GMA was unsuccessful, even at 80 °C and with reaction times of 48 h. The reaction was then tested with various catalysts, such as BFEt [42], TiBuO [43], ETPP [44], DMAP [45].

According to literature suggestions, the temperature was initially set at 40 °C. However, in these conditions no reaction was observed even in the presence of catalysts. Consequently, the influence of the temperature on the reactivity was studied. Eventually it was found that reaction rate markedly increased with increase of the temperature. However, high temperatures should be avoided as they could induce spontaneous polymerization of GMA. Finally, T was set at 80 °C, where satisfactory yields of products were obtained, and no polymerization of GMA occurred.

It is interesting to observe that in all cases, whatever the catalyst used, reaction yielded one major product along with traces of by-products. It was also observed that the reaction progresses similarly, and at the end an equilibrium in product composition was noticed. ^1H NMR analysis showed that the major product did not contain the glyceryl moieties, but the spectrum fitted reasonably with the mono-transesterified product **MA19** (Fig. 1).

Indeed, in such conditions the transesterification product formed through a nucleophilic attack of the hydroxyl of DR19 to the carbonyl of GMA with release of glycidol was the most abundant species, only small amounts of ring-opening derivatives being present. This was observed even with well-known oxirane ring-opening catalysts, such as BFEt and ETPP. In addition, longer reaction times and the use of an excess of GMA led to the formation of the dimethacrylated DR19 at the expense of the mono-methacrylated **MA19**.

The preferential reaction pathway leading to transesterification products was observed in the reaction of GMA with dextran [46], 2-{[2-(dimethylamino)ethyl]methylamino}ethanol [47], 1,4-butanediol [48], hyperbranched polyglycerol [49]. This orientation of the reaction is specific of GMA, and no transesterification was observed for other methacrylate esters [46,48]. The authors explained this result in terms of stabilization of the negative charge over the two oxygen atoms of the glycidol anion, which make the latter an efficient leaving group.

The course of the reaction between DR19 and GMA was found to be dependent on the catalyst nature. Among the tested catalysts, DMAP was demonstrated to be more effective, in terms of both reaction rate and product yield, confirming the results reported in literature [48]. However, although has been claimed that transesterification is possible only using basic catalysts [48], we observed formation of **MA19** in moderate yields also in the presence of a Lewis acid, such as ethyltriphenylphosphonium bromide.

The thermal behaviour of **MA19** and the parent DR19 was investigated by DSC (not shown). DR19 showed a melting peak at 215 °C, whereas **MA19** showed no evidence of melting by means of DSC, however a solid-to-liquid transition was observed at approximately 130 °C by optical microscopy observations. The DSC trace of **MA19** showed only a broad exothermic peak with an onset temperature of 135 °C, due to self polymerization of the acrylic

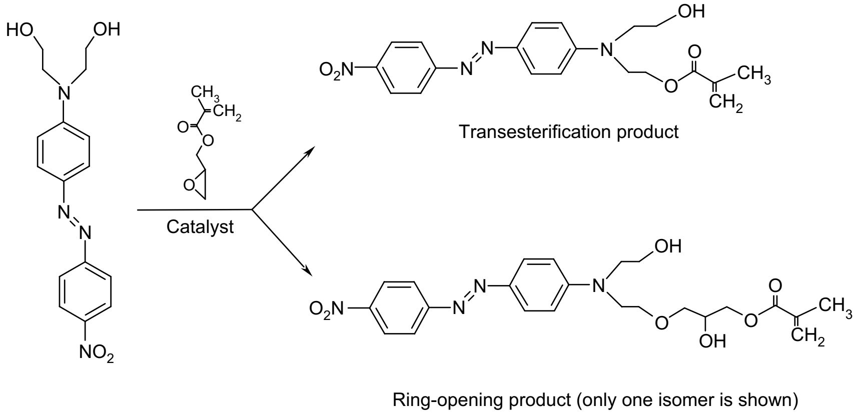

Scheme 1. Expected products in the reaction between DR19 and GMA.

double bonds. It is likely that this highly exothermic reaction hinders the detection of the endothermic melting process.

3.2. Preparation and properties of the copolymers

3.2.1. Molecular weight measurements and chemical characterization

The structure of poly(**CS**–**GMA**–**MA19**) is sketched in Scheme 2. Both poly(**CS**–**GMA**) and poly(**CS**–**GMA**–**MA19**) are well soluble in several organic solvents (acetone, $CHCl_3$, THF, DMF and DMSO) and exhibit good film-forming behaviour. Poly(**CS**–**GMA**) is transparent, while poly(**CS**–**GMA**–**MA19**) was isolated as a red powder.

It was reported that the vinyl monomers carrying chromophores with $-NO_2$ groups are rather difficult to undergo radical polymerization because of the inhibition of these groups [44].

GPC analysis (Table 1) indeed showed that M_n values of the copolymer poly(**CS**–**GMA**–**MA19**) are lower than those observed for poly(**CS**–**GMA**), thus confirming that the nitro-substituted azobenzene chromophore favours chain-transfer reactions during the polymerization [50,51]. The polydispersity (PI) of the polymers is typical of a free radical polymerization process, as evidenced in Table 1, although as expected it is higher for poly(**CS**–**GMA**–**MA19**).

The GPC curves (Fig. 2) of the two copolymers are similar, however poly(**CS**–**GMA**–**MA19**) shows a bimodal pattern of the molecular-mass curve, and consequently the summary molecular mass distribution of this polymer is wider than that of poly(**CS**–**GMA**), due to a higher fraction of lower molecular mass oligomers. This can be also rationalized by the occurrence of the chain-transfer reactions.

Fig. 3 shows the infrared spectra of the two polymers in the region 800–1600 cm^{-1}. Several absorption peaks due to the presence of the azobenzene chromophore are visible. The absorption of the $-NO_2$ group in the side chain chromophore can be identified at 1515 and 1340 cm^{-1}, while peaks appearing at 1140, 1385 and 860 cm^{-1} are due to C–N linkages.

Fig. 4 shows the ^{13}C NMR spectrum of poly(**CS**–**GMA**–**MA19**), which displayed the characteristic chemical shifts of the carbon atoms of the constituting repeat units of the polymer: the signals of chlorostyrene at 143–128 ppm, the weak peaks of **MA19** at 126–111 ppm, the peaks of GMA at 175 and between 65 and 20 ppm.

The relative composition of the copolymers was determined by means of ^1H NMR [40], although the ^1H NMR spectra of the polymers showed a signal broadening. The mole fraction of CS units in the copolymer poly(**CS**–**GMA**) was found to be equal to 0.69, while it was 0.80 in the feeding composition. This change in polymer relative composition with respect to the initial mixture reveals a slight preference of the propagation species of CS for GMA monomers. A similar behaviour was reported for copolymers based on pentafluorostyrene and glycidyl methacrylate, and a lower

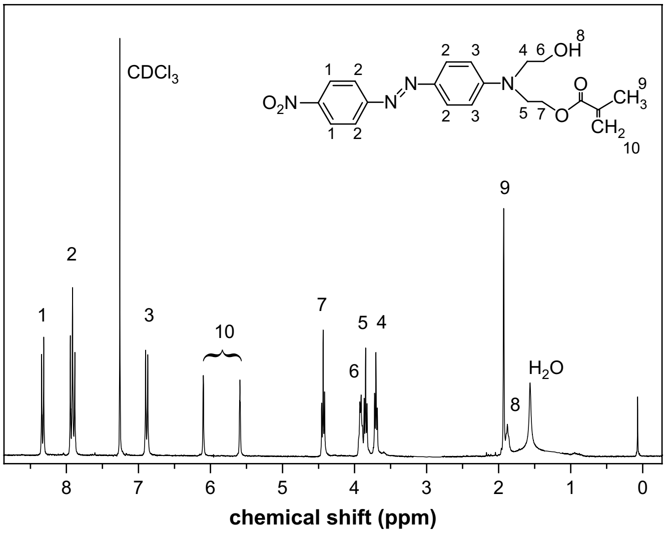

Fig. 1. ^1H NMR spectrum of the monotransesterification product of the reaction between DR19 and GMA.

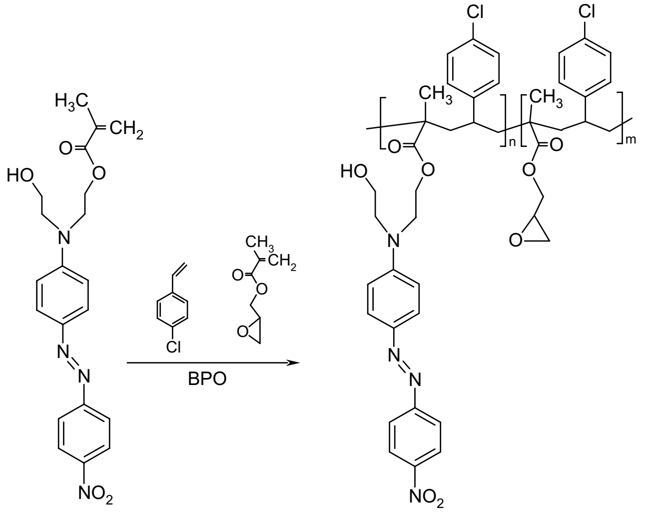

Scheme 2. Reaction route to poly(**CS**–**GMA**–**MA19**).

Table 1
GPC characteristics of poly(**CS–GMA**) and poly(**CS–GMA–MA19**).

Polymer	M_n	M_w	PI
Poly(**CS–GMA**)	28,220	44,218	1.57
Poly(**CS–GMA–MA19**)	18,269	42,607	2.33

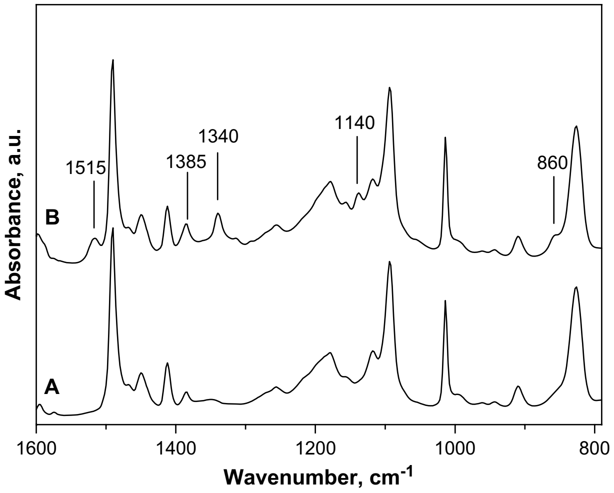

Fig. 3. 1600–800 cm^{-1} region of FTIR spectra of (A) poly(**CS–GMA**) and (B) poly(**CS–GMA–MA19**).

molar fraction of pentafluorostyrene compared to GMA monomer was observed in the polymer with respect to the feeding composition [13].

In the case of poly(**CS–GMA–MA19**), ^{1}H NMR was used to determine the amount of chromophore units, which was grafted onto the copolymer. Therefore, the surface area under the peak at 8.33 ppm, related to the nitroazobenzene residue was compared to that due to the aromatic protons of chlorostyrene. It was found that the molar ratio between CS and **MA19** is approximately 85. Since the molar ratio in the feed was 59, this entails that about 30% of the **MA19** co-monomer was not copolymerized, due to the inhibition ascribed to the $-NO_2$ groups. In terms of net amount of chromophore grafted onto the polymer, the calculated molar amount of MA19 corresponded to a DR19 chromophore to polymer weight ratio of approximately 2%.

3.2.2. Thermal properties and crosslinking degree

DSC analysis of the copolymers showed glass transition at 111.5 °C and 113.5 °C for poly(**CS–GMA**) and poly(**CS–GMA–MA19**), respectively (Table 2). The slightly higher T_g detected for the azo-doped copolymer, which showed lower molecular weight, indicates that the presence of the stiff chromophore directly linked to the polymer backbone is able to hamper the molecular relaxations associated with the glass transition.

In addition, both the uncrosslinked polymers displayed a small peak at the high temperature side of the transition due to the excess enthalpy reached in the glassy state (Fig. 5, only poly(**CS–GMA–MA19**) is shown). Upon rapid heating through T_g, the polymer molecules quickly relax to their equilibrium thermodynamic state, resulting in an apparent excess enthalpy peak [52,53].

Upon crosslinking, the T_g of poly(**CS–GMA–MA19**) increased of about 40 °C, reaching a value of 153 °C (Fig. 5). This confirms the occurrence of crosslinking between epoxy groups, resulting in a polymer network with improved stability. Moreover, the resulting films possess increased solvent resistance after thermal crosslinking, which is highly desirable for multilayer processing in the fabrication of electro-optical devices. Nonetheless, it has to be noticed that a T_g value of 164 °C was observed for the crosslinked poly(**CS–GMA**), suggesting that the crosslinking reaction occurred to a higher extent in the latter polymer. Therefore, the crosslinking degree was determined for both polymers, as it is also of great importance for the macroscopic stability of the orientation. Infrared spectroscopy allowed monitoring the disappearance of the epoxy groups directly involved in the curing reaction (Fig. 6). From an inspection of the spectra, it can be observed that the absorption at 912 cm^{-1} does not disappear completely, which confirms that unreacted epoxy groups are still present even after long curing times.

Since the experimental absorbance was found to be as low as to fall within the validity of the Lambert–Beer relation, the relative conversion α, of the epoxy groups in the investigated system was determined by the following equation:

$$\alpha = 1 - \frac{\overline{A}_t}{\overline{A}_0} \tag{1}$$

where A represents the absorbance, and the subscripts 0 and t denote reaction times zero and t, respectively. For the calculation of α, peak areas have been considered instead of the peak heights. This was done to set more accurate calibrations, since peak areas are

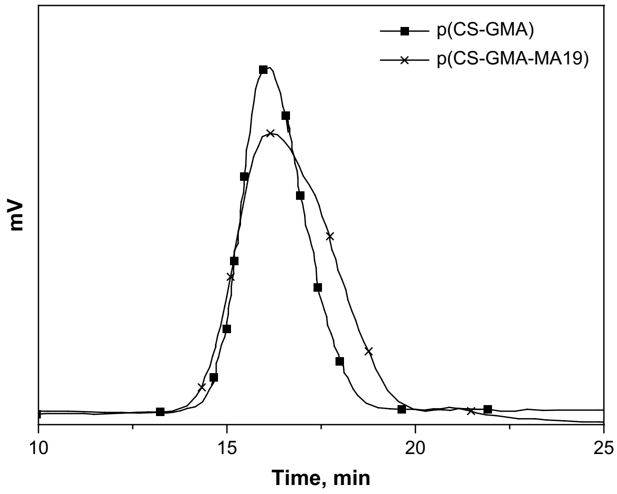

Fig. 2. GPC chromatograms of the polymers poly(**CS–GMA**) and poly(**CS–GMA–MA19**).

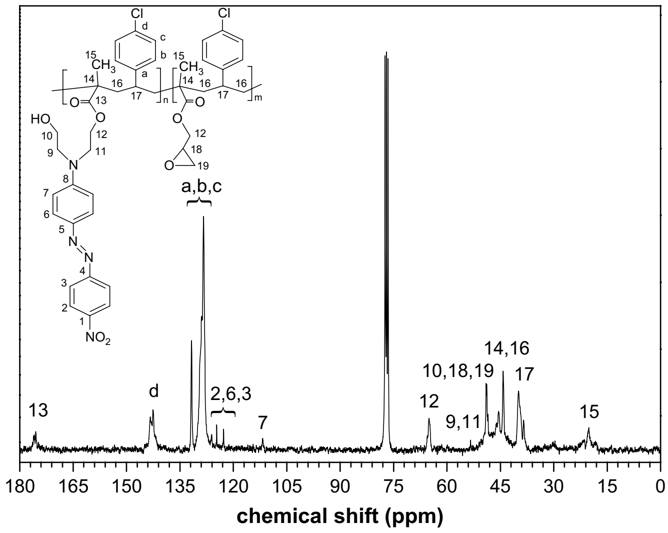

Fig. 4. ^{13}C NMR spectrum of poly(**CS–GMA–MA19**).

Table 2
Thermal properties of poly(**CS–GMA**) and poly(**CS–GMA–MA19**).

Polymer	T_g (°C)	T_{onset}[b] (°C)	T_{max}[c] (°C)	Char yield$_{800}$ (%)
Poly(**CS–GMA**)	111.5 (164.0)[a]	353	400	ND
Poly(**CS–GMA–MA19**)	113.5 (153.1)[a]	363	409	4.5

[a] T_g after crosslinking.
[b] Onset temperature of weight loss.
[c] Temperature of maximum decomposition rate.

measured by adding the absorbance of many different data points together and are not dependent on a single data point [54]. Besides, $\bar{A}$ corresponds to the absorbance of the 912 cm^{-1} peak area of the epoxy ring stretching, corrected for the sample thickness. The thickness correction was accomplished by using the invariant peak at 830 cm^{-1} as an internal standard, corresponding to the out of plane =C–H bending [55].

Fig. 7 shows the curves of the relative conversion of epoxy groups (α) for poly(**CS–GMA**) and poly(**CS–GMA–MA19**). Both the reaction rate and the final conversion degree are significantly lower for poly(**CS–GMA–MA19**), except for the first minutes, in which the conversion rate is the same for both polymers. Poly(**CS–GMA–MA19**) yielded a epoxy groups conversion value of approximately 40% after the photoinitiated crosslinking process at 130 °C, while poly(**CS–GMA**) approached a value of 70%. The incomplete conversion can be explained in terms of hindered segmental motion due to the increasing glass transition temperature upon crosslinking. Besides, in the case of poly(**CS–GMA–MA19**) the presence of the bulky chromophore segment further hinders the molecular mobility of the reacting groups, leading to a still lower α value.

The data related to epoxide conversion, alongside the results obtained by NMR characterization could be exploited to get a rough estimation of crosslinking density and M_c, the average molecular weight between crosslinks.

We have calculated an approximate value of M_c as follows, assuming that all the epoxide groups are statistically distributed along the polymer backbone.

From NMR characterization the ratio between CS and GMA monomers in poly(**CS–GMA**) was found to be equal to 2.33 (see Section 3.2.1), while FTIR analysis showed that about 70% epoxides undergo ring-opening. Assuming that all the reacted epoxy groups form crosslinks, this entails that the number of crosslinks corresponds to 0.35 GMA units, since according to the proposed mechanism the formation of a crosslink requires two epoxy rings to be opened [14]. In turn, this means that one crosslink out of 2.86 epoxy groups should be formed, therefore the average chain segment between consecutive crosslinks should contain 2.86 GMA monomers and 6.66 CS units, as calculated from the CS/GMA ratio obtained from NMR. Consequently, multiplying these values by the respective molecular weights an M_c value of 1330 g/mol is obtained. In the case of poly(**CS–GMA–MA19**) similar considerations account for an M_c value of about 3100 g/mol.

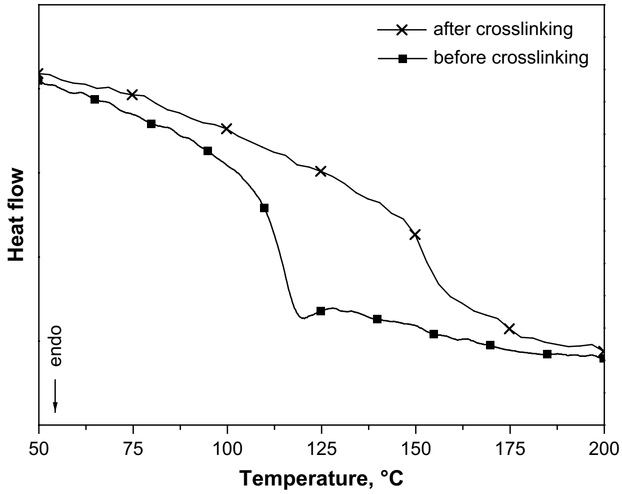

Fig. 5. DSC curves of poly(**CS–GMA–MA19**) before and after crosslinking.

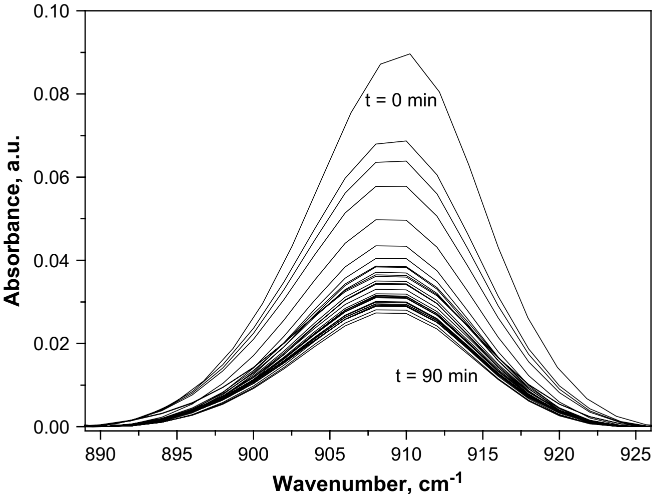

Fig. 6. Evolution of the FTIR spectra of poly(**CS–GMA**) in the region of epoxy ring stretching peak during isothermal cure at 130 °C.

The thermal degradation of the uncrosslinked polymers was studied by TGA in nitrogen. The TGA traces (Fig. 8) show that both polymers have good thermal stability, temperatures of initial decomposition being 353 and 363 °C for poly(**CS–GMA**) and poly(**CS–GMA–MA19**), respectively (Table 2). The observed values are in a good agreement with literature data related to poly(CS) [56], while poly(GMA) is known to start degrading at lower temperatures [31,34]. This result, alongside the observation that the degradation process occurs in a single weight-loss step, suggests that chlorostyrene moieties enhance the thermal stability of glycidyl methacrylate segments. This behaviour has been already observed for copolymers of fluorostyrene and glycidyl methacrylate [13].

It is also to underline that poly(**CS–GMA–MA19**) shows a higher thermal stability compared to poly(**CS–GMA**). It was observed that polymers containing chromophore groups very similar to that contained in poly(**CS–GMA–MA19**) in both main and side chains [23,31,39,57,58], decompose at temperatures associated with the decomposition of chromophore, generally lowering the polymer thermal stability.

In the present case, the presence of the nitroazobenzene substituent improved the stability of the copolymer. The mechanism of the thermal degradation of the copolymer under examination most probably involves the formation of radical species, which can propagate the chain reaction in a so-called unzipping depolymerization [56,59]. In this framework, any species able to hinder radical transfer processes could enhance the thermal stability of the polymer. In literature several reports evidence the possibility of intramolecular electron transfer with the formation of relatively stable radical anion on pendant *p*-nitroazobenzene molecules [60–62]. Therefore, the DR19 chromophore can act as

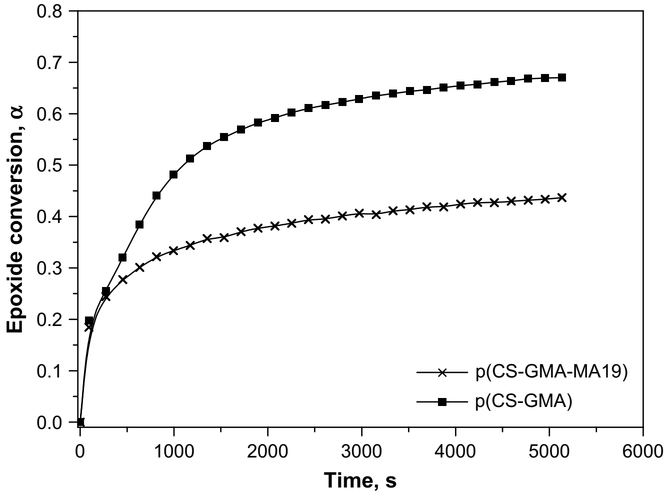

Fig. 7. Relative conversion of epoxy groups, α, for poly(**CS–GMA**) and poly(**CS–GMA–MA19**) at 130 °C. Lines are theoretical fit of the experimental data.

a radical scavenger, thus retarding the propagation of the radical chain reaction that causes the unzipping of the polymer backbone.

3.3. Optical characterization

The UV–vis spectrum of DR19 measured in acetone (Fig. 9) showed an absorption peak at $\lambda_{\max} = 484$ nm attributed to the $n \rightarrow \pi^*$ transitions of the azobenzene group [50,63]. Compared to the UV spectrum of DR19, the absorption of **MA19** was blue-shifted, exhibiting a peak at 463 nm. This hypsochromic effect is likely related to site-isolation effects due to the acrylic moieties, which can decrease intermolecular electrostatic interaction between the chromophores [30].

Poly(**CS–GMA–MA19**) displayed an absorption band at 468 nm, both when it was analysed as an acetone solution and when a polymer film was investigated. In both cases, higher absorbance values compared to DR19 and MA19 are visible in the near-UV region, due to the tail of the absorption from the chlorostyrene moieties. The spectrum obtained on a polymer film also shows fringing effects, which originate from interference of the light beam from the parallel surfaces of the sample.

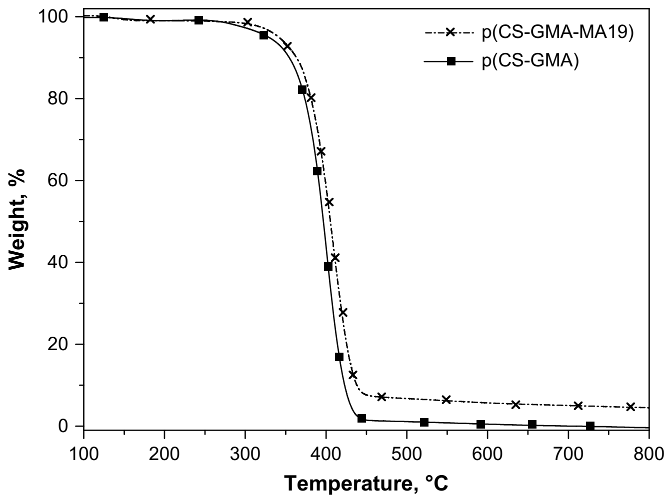

Fig. 8. Thermogravimetric curves for poly(**CS–GMA**) and poly(**CS–GMA–MA19**) in nitrogen, 10 °C/min.

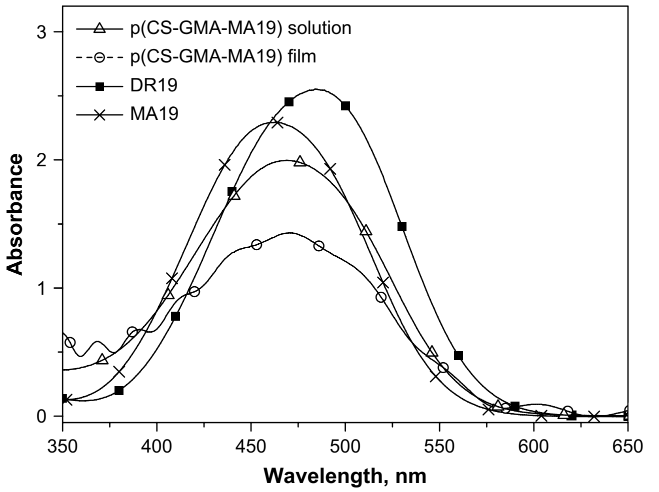

Fig. 9. UV–visible absorption spectra of DR19, MA19, poly(**CS–GMA–MA19**) measured in acetone, and poly(**CS–GMA–MA19**) film measured on a fused silica slide.

One of the most important optical parameters of a material is its refractive index. Such a value also allows defining the potential application in different fields of interest. To measure the refractive index of our material we used a traditional technique (*m-line technique*), involving the light propagation in a planar waveguide coupled by a prism, which is very easy to perform but requires the preparation of thin films of the considered material spun on a substrate. The prism coupler provides a fast, accurate and reliable method of determining refractive index and thickness of thin dielectric films. Films have been spin-coated onto fused silica substrates and characterised by the prism coupling method to determine the refractive index and the thickness. If the conditions for coupling a light beam at a prism-film interface in a total internal reflection (TIR) regime are satisfied, a modal propagation occurs into the planar waveguide. The number of modes propagating depends on the thickness of the core and, as well known, the selection of the single mode occurs by the variation of the incident angle of the light beam at the prism face. Such a method allows one to selectively excite a particular mode of the waveguide. The effective mode indices N_m and the propagation constant β_m are inter-related through:

$$\beta_m = |\vec{k}|N_m = |\vec{k}|n_\mathrm{f}\sin\theta_m \tag{2}$$

where the subscript m refers to the mth order guided mode, θ_m is the mode excitation angle measured normal to the incident face of the prism, k is the wave vector and n_f is the refractive index of the film. The importance of N_m lies in the fact that it allows the film index and/or thickness to be determined through the modal conditions. For a single mode waveguide either the thickness or the refractive index must be known in order to calculate the other. If there are two modes present, then both the index and thickness may be determined from the two effective indices N_m. When more than two modes are observed, then the technique becomes self-consistent. The coupling angle which excites each mode is obtained by measuring the angle of incidence on the prism entrance face for which the mth mode is excited. A computational routine for the PC was used for evaluating the linear refractive indices and thickness of the guiding layer, based on the above method.

We performed measurements on poly(**CS–GMA–MA19**) films, with different thicknesses ranging from 1 to 1.4 μm. These measurements were carried out at 632.8 nm using a He–Ne laser beam, TE polarized and TM polarized, on three differently prepared

Table 3
Summary of the optical parameters (refractive indices and thicknesses) of three planar waveguides realized based on poly(**CS–GMA–MA19**).

Materials	Refractive indices@632.8 nm			Thickness (μm)
	n_{TE}	n_{TM}	Δn	
WG1	1.5842	1.5918	0.0076	1.37 ± 0.02
WG2	1.5827	1.5882	0.0055	1.32 ± 0.02
WG3	1.5825	1.5898	0.0073	1.17 ± 0.02

waveguides. The refractive index of the substrate (silica fused) is 1.4570 and the prism index is 1.7561 at the same wavelength. The prism angle between the incident face and the prism is 60.13°.

The calculated values of the refractive indices for the three waveguides with different thickness are reported in Table 3. The estimated average refractive index value of the poly(**CS–GMA–MA19**) is $\boldsymbol{n}_{\mathbf{TE}} = 1.5831 \pm 0.0005$ for the TE polarised light, $\boldsymbol{n}_{\mathbf{TM}} = 1.5901 \pm 0.0005$ for the TM polarised light, with an optical anisotropy of 0.007 ± 0.001.

4. Conclusion

A photochemically crosslinkable copolymer of chlorostyrene (CS) and glycidyl methacrylate (GMA) containing chemically bonded pendant azobenzene groups was synthesized and characterized.

A novel monomer (MA19) derived from reaction between GMA and Disperse Red 19 (DR19) was first prepared and characterized. The reaction between GMA and DR19 specifically yielded trans-esterification products, traces of epoxy ring-opening species being present. The monomer was successfully copolymerized with CS and GMA to obtain the dye-modified copolymer, whose chemical and chemico-physical characteristics were compared to those of a plain CS-co-GMA copolymer. A decrease in polymerization degree was observed when MA19 was copolymerized with CS and GMA. NMR spectroscopy indicated that about 30% of the azo modified monomer was not copolymerized, due to the inhibition ascribed to the pendant $-NO_2$ groups. It was also observed that the presence of grafted DR19 affected to some extent the crosslinking reaction, as a lower epoxy group conversion was observed for the modified copolymer. Thermal analysis indicated that the copolymer containing DR19 showed increased thermal stability.

The new copolymer was employed to prepare by spinning technique planar waveguides of different thicknesses, which are suitable to applications in several fields of interest such as photonics and telecommunication systems, electro-optical devices and sensors. A preliminary characterization of the prepared waveguides was carried out by *m-line* spectroscopy to measure the refractive indices and the thicknesses of the samples. The refractive index at 632.8 nm was measured for TE and TM polarized light on three differently prepared waveguides, and the samples were found to be optically anisotropic.

The characterization of the proposed materials, their processability and their chemical structure indicate that they are very good candidates for preparing optical waveguides. The interest on these materials as active elements could be further extended according to their electro-optical properties. Such a study is in progress.

Acknowledgements

The authors thank Mr. Giustino Orefice (ICTP-CNR) for assistance in performing FTIR measurements, Mr. Salvatore Zambardino (ICB-CNR) for performing NMR experiments, and Dr. Raniero Mendichi (ISMAC-CNR) for GPC analysis.

References

[1] Pei Q, Yu G, Zhang C, Yang Y, Heeger AJ. Science 1995;269:1086–8.
[2] Heeger AJ. Solid State Commun 1998;107:673–9.
[3] Akcelrud L. Prog Polym Sci 2003;28:875–962.
[4] Prasad PN, Williams DJ. In: Prasad PN, Paras N, editors. Introduction to nonlinear optical effects in molecules and polymers. New York: Wiley; 1991 [chapters 7–10].
[5] Kaino T, Tomaru S. Adv Mater 1993;5:172–8.
[6] Koeppen C, Yamada S, Jiang G, Garito AF, Dalton LR. J Opt Soc Am B 1997;14:155–62.
[7] Adronov A, Gilat SL, Frechet JMJ, Ohta K, Neuwahl FVR, Fleming GR. J Am Chem Soc 2000;122:1175–85.
[8] Kaino T. Appl Phys Lett 1986;48:757–8.
[9] Taino N, Koike Y. Polym J 2000;32:43–50.
[10] Booth BL. In: Hornak LA, editor. Polymers for lightwave and integrated optics: technology and applications. New York: Marcel Dekker; 1992. p. 231.
[11] Hartman DH. In: Hornak LA, editor. Polymers for lightwave and integrated optics: technology and applications. New York: Marcel Dekker; 1992. p. 267.
[12] Eldada L, Blomquist R, Shacklette LW, McFarland MJ. Opt Eng 2000;39:596–609.
[13] Pitois C, Vukmirovic S, Hult A, Wiesmann D, Robertsson M. Macromolecules 1999;32:2903–9.
[14] Pitois C, Hult A, Wiesmann D. J Opt Soc Am B 2001;18:908–12.
[15] Hermann DS, Scalia G, Pitois C, De Marco F, D'Havé K, Abbate G, et al. Opt Eng 2001;40:2188–98.
[16] Tkachenko V, Marino A, Vita F, D'Amore F, De Stefano L, Malinconico M, et al. Eur Phys J E 2004;14:185–92.
[17] Gudipati CS, Tan MBH, Hussain H, Liu Y, He C, Davis TP. Macromol Rapid Commun 2008;29:1902–7.
[18] Brasselet S, Zyss J. J Opt Soc Am B 1998;15:257–88.
[19] Dumont M. Mol Cryst Liq Cryst 1996;282:437–50.
[20] Wyman GM. Chem Rev 1955;55:625–57.
[21] Xie S, Natansohn A, Rochon P. Chem Mater 1993;5:403–11.
[22] Oliveira ON, dos Santos DS, Balogh DT, Zucolotto V, Mendonça CR. Adv Colloid Interface Sci 2005;116:179–92.
[23] Shulyndin SV, Vakhonina TA, Estrina GA, Rozenberg BA, Zuev MB. Polym Sci Ser A 2007;49:782–94.
[24] Ji S, Li Z, Zhou X, Cao M, Dai D, Zhang R, et al. Polym Adv Technol 2003;14:254–9.
[25] Houa A, Liu H, Sun J, Zhang D, Yi M. Opt Laser Technol 2007;39:411–4.
[26] Tan J, Li AD, Fan XZ, Liu WC, Xu ZX, Lin Y, et al. Phys Stat Solidi A 2007;204:1114–22.
[27] Barto RR, Frank CW, Bedworth PV, Taylor RE, Anderson WW, Ermer S, et al. Macromolecules 2006;39:7566–77.
[28] Hasegawa M, Ikawa T, Tsuchimori M, Watanabe O. J Appl Polym Sci 2002;86:17–22.
[29] Hayakawa T, Horiuchi S, Shimizu H, Kawazoe T, Ohtsu M. J Polym Sci Part A Polym Chem 2002;40:2406–14.
[30] Xie J, Deng X, Cao Z, Shen Q, Zhang W, Shi W. Polymer 2007;48:5988–93.
[31] Bosc D, Foll F, Boutevin B, Rousseau A. J Appl Polym Sci 1999;74:974–82.
[32] Wang Y, Wang X, Chuai X, Fu N, Cui Z, Yi M, et al. Polym Int 2004;53:1106–12.
[33] Navarro-Rodriguez D, Rodriguez-Gonzalez FJ, Romero-Garcia J, Jimenez-Regalado EJ, Guillon D. Eur Polym J 1998;34:1039–45.
[34] Zhang L, Cai Z, Yu Q, Liang Z. J Appl Polym Sci 1999;71:1081–7.
[35] Wan Rosli WD, Kumar RN, Mek Zah S, Hilmi MM. Eur Polym J 2003;39:593–600.
[36] Jones RJ, Cordina GPG, Murphy JJ. J Mater Chem 1997;7:421–7.
[37] Udagawa A, Yamamoto Y, Inoue Y, Chujo R. Polymer 1991;32:2779–84.
[38] Crivello JV, Acosta Ortiz R. J Polym Sci Part A Polym Chem 2001;39:3578–92.
[39] Chen M, Yu L, Dalton LR, Shi Y, Steier WH. Macromolecules 1991;24:5421–8.
[40] Brar AS, Yadav A, Hooda S. Eur Polym J 2002;38:1683–90.
[41] Lee JY, Shim MJ, Lee HK, Kim SW. J Appl Polym Sci 2001;82:2372–80.
[42] Guivisdalsky PN, Bittman R. J Am Chem Soc 1989;111:3077–9.
[43] Yatluk YG, Suvorov AL, Khrustaleva EA, Chernyak SV. Russ J Org Chem 2004;40:769–72.
[44] Zhang LZ, Li Y, Liang ZX, Yu QS, Cai ZG. React Funct Polym 1999;40:255–62.
[45] Van Dijk-Wolthuis WNE, Franssen O, Talsma H, van Steenbergen MJ, Kettenes-van den Bosch JJ, Hennink WE. Macromolecules 1995;28:6317–22.
[46] Van Dijk-Wolthuis WNE, Kettenes-van den Bosch JJ, van der Kerk-van Hoof A, Hennink WE. Macromolecules 1997;30:3411–3.
[47] Findlay PH, Sherrington DC. Macromolecules 1999;32:5970–2.
[48] Derouet D, Nguyen GTM, Brosse JC. Eur Polym J 2002;38:2017–21.
[49] Oudshoorn MHM, Rissmann R, Bouwstra JA, Hennink WE. Biomaterials 2006;27:5471–9.
[50] Angiolini L, Caretti D, Giorgini L, Salatelli E, Altomare A, Carlini C, et al. Polymer 2000;41:4767–80.
[51] Hayashi A, Goto Y, Nakayama M, Kaluzynski K, Sato H, Kato K, et al. Chem Mater 1992;4:555–62.
[52] Marshall AS, Petrie SEB. J Appl Phys 1975;46:4223–30.
[53] Fried JR, Karasz FE, MacKnight WJ. Macromolecules 1978;11:150–8.
[54] Smith BC. Quantitative spectroscopy: theory and practice. San Diego: Academic Press; 2002. p. 64–7.
[55] Ambrogi V, Giamberini M, Cerruti P, Pucci P, Menna N, Mascolo R, et al. Polymer 2005;46:2105–21.

[56] Bertini F, Audisio G, Kiji J. J Anal Appl Pyrolysis 1994;28:205–17.
[57] Shulyndin SV, Vakhonina TA, Ivanova NV, Gubanov EF, Ustyugov AN, Fominykh OD, et al. Polym Sci Ser A 2005;47:808–19.
[58] Yu D, Gharavi A, Yu L. J Am Chem Soc 1995;117:11680–6.
[59] Peterson JD, Vyazovkin S, Wight CA. Macromol Chem Phys 2001;202:775–84.
[60] Zhao C, Horiuchi H, Okutsu T, Tobita S, Takigami S, Hiratsuka H. Bull Chem Soc Jpn 2003;76:961–9.
[61] Monti S, Flamigni L. J Phys Chem 1986;90:1184–6.
[62] Itoh T, McCreery RL. J Am Chem Soc 2002;124:10894–902.
[63] Lee JK, Park SW, Lee JW, Kim MR. Polym Int 2006;55:849–53.